



ISSN: 0067-2904

Improve The Fully Convolutional Network Accuracy by Levelset and The Deep Prior Method

Samera Shams Hussein^{1*}, Sukaina Sh Altyar², Inas Ali Abdulmunem³

¹Department of Computer Science, College of Education for pure Science, University of Baghdad, Baghdad, Iraq

²Department of Computer Science, College of Education for pure Science, University of Baghdad, Baghdad, Iraq

³Department of Computer science, College of Science University of Baghdad, Baghdad, Iraq

Received: 2/6/2022

Accepted: 28/11/2022

Published: 30/5/2023

Abstract

Deep learning techniques allow us to achieve image segmentation with excellent accuracy and speed. However, challenges in several image classification areas, including medical imaging and materials science, are usually complicated as these complex models may have difficulty learning significant image features that would allow extension to newer datasets. In this study, an enhancing technique for object detection is proposed based on deep conventional neural networks by combining levelset and standard shape mask. First, a standard shape mask is created through the "probability" shape using the global transformation technique, then the image, the mask, and the probability map are used as the levelset input to apply the image segmentation. The test results show that when using the proposed method with DCNN, it can achieve a close segmentation area and extract features with higher detail than traditional segmentation. The proposed model achieved 94.43% in precision and 95.91% in recall %, so it got 95.16% in F1-score. When comparing the proposed model with the same CNN model without Levelset, the result shows that the proposed model achieved accuracy of 0.951, which is higher than CNN model without Levelset that achieved 0.902.

Keywords: LevelSet, global affine transformation, convolutional neural network.

تحسين دقة الشبكة التلافيفية الكاملة عن طريق دمج خوارزمية خط المستوى وطريقة التعلم العميقة المسبقة

سميره شمس حسين^{1*}, سكينه شكري محمود², ايناس علي عبدالمنعم³

¹قسم علوم الحاسبات، كلية التربية للعلوم الصرفة/ابن الهيثم، جامعة بغداد، بغداد، العراق

²قسم علوم الحاسبات، كلية التربية للعلوم الصرفة/ابن الهيثم، جامعة بغداد، بغداد، العراق

³قسم علوم الحاسوب، كلية العلوم، جامعة بغداد، بغداد، العراق

*Email: Samera.s.h@ihcoedu.uobaghdad.edu.iq

الخلاصة

تسمح تقنيات التعلم العميق بالحصول على تجزئة الصورة بدقة وسرعة ممتازين. ومع ذلك، فإن التحديات في العديد من مجالات تصنيف الصور، بما في ذلك التصوير الطبي وعلوم المواد، عادة ما تكون صعبة نظرًا لأن هذه النماذج المعقدة قد تكون قد حصلت على ميزات صور مهمة صعبة التعلم والتي من شأنها أن تسمح بالامتداد إلى مجموعات البيانات الأحدث. في هذه الدراسة، تم اقتراح تقنية محسنة لاكتشاف الكائنات القائمة على الشبكة العصبية التقليدية العميقة من خلال مجموعة المستوى المدمجة وقناع الشكل القياسي. أولاً، يتم إنشاء قناع شكل قياسي من خلال شكل "الاحتمالية" باستخدام تقنية التحويل الأفيني العالمي (GAT)، ثم تم استخدام الصورة والقناع الأفيني وخريطة الاحتمال كمدخل مجموعة المستوى لتطبيق تجزئة الصورة. تظهر نتائج الاختبار أنه عند استخدام الطريقة المقترحة مع DCNN، يمكنها تحقيق منطقة تجزئة قريبة جدًا واستخراج ميزة مع صورة عالية التفاصيل من التجزئة التقليدية. أظهرت النتائج ان النموذج المقترح حصل على 94.43% في الدقة (precision) و 95.91% في نسبة الاسترجاع (recall)، وبالنتيجة حصل على 95.16% في مقياس (F1-score). عند مقارنة النموذج المقترح مع نفس طراز CNN بدون Levelset، تظهر النتيجة أن النموذج المقترح حقق دقة أعلى بلغت 0.951 أي أكثر من نموذج CNN بدون Levelset الذي حقق 0.902.

1. Introduction

Recently, machine learning (ML) methods have played a significant role in dealing with big problems in a smart and effective way. ML methods can solve immense problems by analyzing massive amounts of data. Furthermore, deep learning techniques, mainly Deep Convolutional Neural Networks (DCNN), have been efficiently used in object detection[1], image classification[2], and caption creation[3]. CNN achieved better performance when compared with shallow and classical networks with hand-crafted features. The process of recognition can be divided into two stages. The first stage is feature extraction and is utilized to minimize data dimensionality for segmented or raw data. The second is the classification stage. A pre-processing stage, ahead of feature extraction that may be needed for filtering the data from noise as well as data segmentation [4].

Image segmentation represents a significant task in computer vision. It is one of the earliest and most researched problems in the field [5]. Many of the conventional approaches to image segmentation depend on the local or global statistical information of a single image [6]. In addition, the segmentation process of an image to get the specific regions typically depends on pre-defined statistical presumptions. Hence, the methods-based threshold techniques can adaptively identify the threshold grayscale depending on the local and global grayscale histogram of an image [6]. Additionally, edge-based approaches depend on 'the areas in the image that individually identify the edges, and these methods have been used to identify the edges to determine the segmentation areas [6]. The final segmentation areas are created using region-based techniques that joins and divides identical regions.

Graph-based techniques use the structure of the graph for representing images and then slice connections of the graph to indirectly obtain image segmentation [7]. The mean shift strategy, which projects most points towards the high-dim feature space and separates the regions based on mean shift clustering, is another option. [8]. The segmentation method based on active contour modeling affects the targeted contour implicitly or explicitly, and the target can be acquired by reducing the energy function. Another segmentation method is adaptive active contours [9].

However, these conventional methods are considered unsupervised methods because they depend on artificially specified patterns instead of patterns learned using the label segmentation

results. More advanced than the conventional methods, there are deep learning approaches that are more likely for locating patterns in images throughout the training set [10].

Due to their effective capacity in high-level features representation, the image segmentation process in deep neural networks (DNNs) is enlarged to semantic segmentation by segmenting areas utilizing sophisticated high-level semantic details [11]. The class of each pixel in the photos is predicted by deep learning methods for image segmentation [12]. To achieve this dense prediction, fully convolutional networks (FCN) enhance the network's fully connected layers with the convolutional layers.

However, no prior shape, boundary roughness, and noise are disadvantages of deep learning algorithms for image segmentation [13]. The FCNs inference mechanism is merely a feedforward procedure, and each pixel's most recent output is only significant for the receptive region. The corresponding receptive field from each pixel's output can span the entire image thanks to the current network layout, which is exceedingly deep [14]. Typically, the semantic information exhibited by the neural network's output improves as these layers become deeper [15]. Additionally, the output layer is at the rear of all layers, which makes the FCN output based upon a high-level view of the image, so this high-level view helps make the output of the FCN at the test set be subjected to the several types of scenarios dealt with in the training set.

In addition, in the case where the scene is complicated, every pixel's output is uncertain. That is shown in several small aspects and tiny objects with wrong outputs. As a result, it is important to make every pixel's output not just depend on the higher semantics of the higher receptive area, but additionally on the low semantics of the small-sized receptive field [16]. According to this rule, recurring networks were proposed utilizing cross-layer connections together with feature pyramid networks having multiscale features. Furthermore, an enhanced network structure search approach for semantic segmentation were suggested. However, these approaches make the models more complicated, and the capability of the model will be limited if the scene becomes complicated [17].

Levelset approaches are becoming commonly used for catching interface evolution, mainly in cases where the interface undergoes intensive topological improvements, joining or pinching off. The levelset application is for a broad range of problems involving computer vision, fluid mechanics, materials science, and combustion, but the main fields that utilize levelset approaches are for image segmentation [18].

2. Related Works

Hu et al. [19] proposed a model-based deep levelset network for the detection of salient objects. They made use of the levelset principle to refine the saliency maps. In addition, they utilized super-pixel filtering to help with the refinement. As their method works only with saliency maps, it is difficult to use in multiclass and multi-object images.

Le et al. [20], introduced an approach combining Variation levelset (VLS) with deep learning by utilizing a new trainable model known as Deep Recurrent levelset (DRLS). The suggested DRLS model consists of three layers : Convolutional layers, levelset layers and Deconvolutional layers having skip connections. The model was used for Brain tumor images segmentation, which are supposed be instantaneous to demonstrate the proposed DRLS performance. The convolutional layer used to learn the visual description of brain tumors at various scales. Given that brain tumor occupies a tiny section of the image, deconvolutional layers have been developed by using skip connections to achieve a higher quality feature map.

Levelset Layer makes the contour in the direction of the brain tumor. For every step, the Convolutional Layer is provided with the levelset map to achieve the feature map of brain tumor. The DRLS model enhances both segmentation accuracy and computational time in comparison with the classic VLS-based approach.

The Contextual Recurrent levelset (CRLS) model was suggested by Le [21]. In their work, the levelset approach was reformulated to be a recurrent neural network, while the curve evolution was presented in a time series. Due to the levelset approach being rarely utilized in multi-class images, they made use of an object detection network to achieve single object images. However, as this method requires an auxiliary network, their work enhanced the performance with no further architectural or network changes.

Kim et al. [22], proposed a new loss function known as the levelset loss that was developed to refine spatial aspects of segmentation results. To handle numerous classes within an image, they first break down the ground truth to binary images. However, every binary image involves background and areas that belong to a class, so it should be converted from levelset functions to class probability maps and compute the energy for every class. The network was trained to reduce the weighted sum of the levelset loss together with the cross-entropy loss. The suggested levelset loss enhances the spatial aspects of segmentation results in both memory and time efficiency. Moreover, the results prove that the proposed model achieves better performance compared with previous approaches.

3. Levelset Method Concept

Levelset Method is widely used in image segmentation because it can handle complex shapes and changes in topology. The idea is to make contours zero-level by defining an implicit function present in a higher dimension. The levelset function is simply a partial differential equation derived from a Lagrangian version of the active contour model.

However, the earlier partial differential equation-driven levelset approaches rely on edge information and are typically noise-sensitive. Thus, the Variation levelset Methods were introduced to address this difficulty by directly deriving the evolutionary partial differential equation from a given energy function. Additional details such as region and shape can be easily and naturally formulated in the levelset domain using new methods. Iteratively applying gradient descent to reduce the evolution energy can solve the levelset based segmentation problem. Even though the variation levelset segmentation problem is non-convex, Chan and Vese found that using well-initialized levelset and momentum-based learning algorithms in neural network training can assist in reaching an optimal outcome. Because of these characteristics, variation levelset approaches can be used in conjunction with deep networks to address binary segmentation problems.

The levelset approach captures the numerical evolution of an implicit interface as the zero contour of the levelset function (ϕ): is defined as the signed distance function given the computational domain \mathbb{R}^n and an interface [23].

$$\phi(x) = \begin{cases} -d & x \in \Omega^- \\ +d & x \in \Omega^+ \\ 0 & x \in \Gamma \end{cases} \quad (1)$$

where d represent the Euclidean distance between x to Γ , and Ω^- is the resulting inside region and Ω^+ is the resulting outside region within the partitioned domain areas.

Supposing that the phase motion $\Omega(t)$ moves with velocity field $v(t, x)$ with boundary $\Gamma(t) : = \partial\Omega(t)$, the evolution of the LSM $\phi(x)$ satisfies:

$$\phi_t + v \cdot \nabla \phi = 0 \quad (2)$$

This equation requires being solved locally near the interface. It is useful to make interfaces that are equal to 1 similar to the signed range. This means that the levelset is a smoothly varying method that is suitable for high-order reliable numerical methods. The reinitialization algorithms preserve the signed range property through solving the steady state case.

The formula is: In practice, a signed distance function (x, y) is preferred since it delivers reliable numerical results. The viscosity solution of the Eikonal equation is also known as a signed distance function, and it meets the uniform gradient condition $= 1$. However, as it deteriorates numerically and wanders away from its desirable signed distance form, noisy features emerge, which are magnified when employed in partial derivative approximation. As a result, frequent reinitialization into a signed distance function is standard. The levelset reinitialization equation was first proposed by [23]:

$$\phi_t + S(\phi_0)(|\nabla\phi| - 1) = 0 \tag{3}$$

Where, ϕ_0 is the levelset function prior to reshaping, and $S(\phi_0)$ is a smoothed-out sign function, and t is the pseudo time. The $S(\phi_0)$ can numerically approximated [24] as:

$$S(\phi_0) = \frac{\phi_0}{\sqrt{\phi_0^2 + (\Delta x)^2}} \tag{4}$$

The zero-LS (Γ), of a bivariate function, $\phi(x): \mathbb{R}^2 \rightarrow \mathbb{R}$, traveling across a discretized domain (Ω), is depicted in Figure 1.

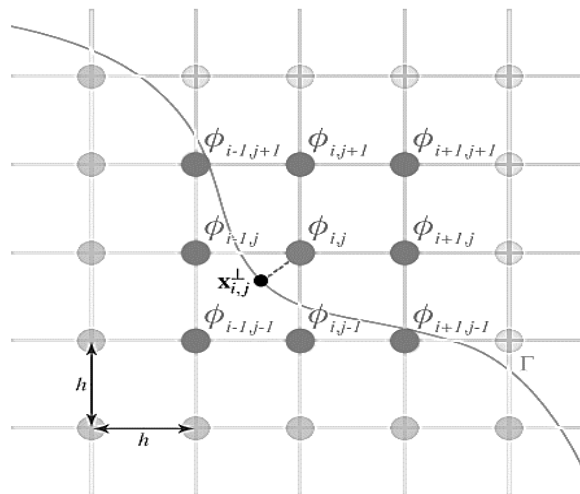


Figure 1: Levelset values are utilized in the normal curvature computation at a grid node $\phi_{(i,j)}$. The normal projection onto the interface (Γ) is denoted by the point $(x_{(i,j)}^\perp)$.

It also displays the nine parameters (φ) used in the numerical estimation of mean curvature at each node (I, j) . To solve equation 3 to a steady state, the fifth-order appropriate Hamilton-Jacobi WENO scheme is used [25] to calculate the spatial derivatives in equations 2 and 3. Geometrical quantities are generally computed from the LS function, involving the unit normal.

$$\vec{N} = \frac{\nabla\varphi}{|\nabla\varphi|} = \frac{\varphi_x^2 \ vbc - 2\varphi_x\varphi_y\varphi_{xy} + \varphi_y^2\varphi_{xx}}{(\varphi_x^2 + \varphi_y^2)^{3/2}} \tag{5}$$

and the curvature,

$$k = \nabla \cdot \left(\frac{\nabla\varphi}{|\nabla\varphi|} \right) = \nabla \cdot \left(\frac{\varphi_x^2 \ vbc - 2\varphi_x\varphi_y\varphi_{xy} + \varphi_y^2\varphi_{xx}}{(\varphi_x^2 + \varphi_y^2)^{3/2}} \right) \tag{6}$$

When the denominators are nonzero, the spatial derivatives in equations 5 and 6 can be calculated using standard second-order accurate central difference. Aside from that, a one-sided difference is used.

From both a theoretical and numerical standpoint, the LSM has been an extremely useful framework. It allowed for the robust description of major changes in domains (including topological changes). From shape optimization techniques, it is possible to determine the shape gradient related to shape Ω , where the vector field $V_\Omega : \mathbb{R}^d \rightarrow \mathbb{R}^d$ such that $J((I_d + tV_\Omega)(\Omega))$ is less than $J(\Omega)$, for $t > 0$ is less enough.

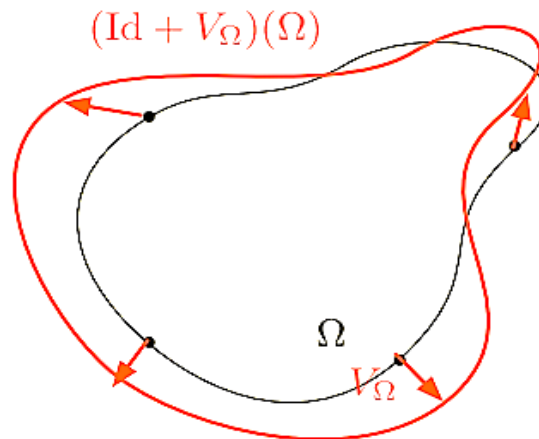


Figure 2: Shape adjusting using LS.

Related to the initial design Ω_0 , the shape sequence can be computed by:

$$\Omega^{n+1} = (I_d + t^n V_{\Omega^n})(\Omega^n) \tag{7}$$

where t^n is a pseudo-time step, evolves by decreasing the criterion $J(\Omega)$.

4. Proposed Model

The levelset with the deep prior procedure is proposed for improving performance of the fully convolutional network and conducting complex sense segmentation using the levelset method. Figure 3 shows the main system scheme.

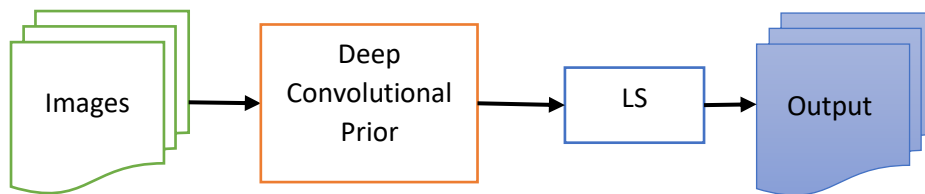


Figure 3: Proposed system scheme.

4.1 Modeling the Deep Conv. Prior

A CNN-based prior is the Deep Convolutional Prior. The proposed CNN is approached as a network having two parts: classification and regression (Figure 4). The categorization part is responsible for identifying the objects within the image. The regression part is used to forecast where each object will be in relation to its bounding box.

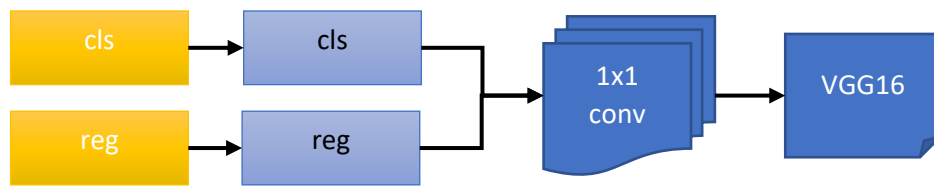


Figure 4: Deep Convolutional Prior structure.

A fully convolutional network can extract desired features and learn patterns during training on the training set, and these capabilities are reflected in the probability map. As a result, based on the pixels in the receptive area, the probability map keeps the details of the segmentation target. The probability map can, for example, reflect the probability that each pixel in the Portrait data set corresponds to a person. Even though there is a chance that it is inaccurate, it preserves most of the correct forecasts, including the correct pattern information. The method of combining the probability map with the shape priors and, the levelset approach for semantic segmentation can be used based on these qualities of the probability map.

The output of the Fully Convolutional Network is a probability map indicating which category every pixel belongs to. The probability map's segmentation form is noisy, but it still preserves a large portion of the proper segmentation. As a result, using the graph attention network approach, an optimum affine transformation of the image's standard shape mask (the shape prior) can be derived based on the "probability" shape. Finally, to accomplish image segmentation, the image, probability map, and affine mask are utilized as inputs to the levelset technique. The proposed model connected layer is shown in the Figure 5.

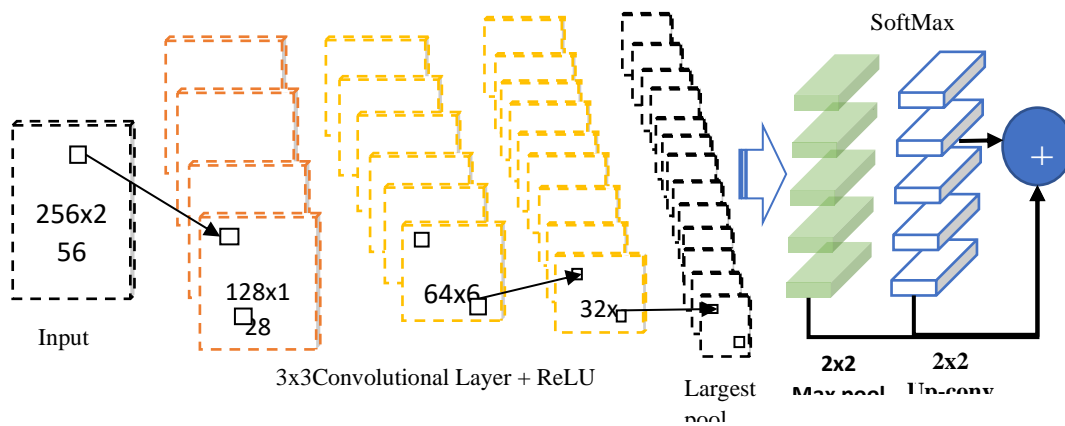


Figure 5: Proposed system scheme.

4.2 The Methodology for Improving Levelset Segmentation

The region force is determined by a reference to the probability that is returned by the classifier. The edge field can depend on this classifier to reduce spurious edges. The levelset technique relies on its accuracy. Nonetheless, a classifier's accuracy is determined by the quality of its training data, and a lack of high-quality training data is evident at the outset. However, it is arguable that the levelset method's posterior probabilities are more accurate than the classifier's initial likelihoods since the posterior probabilities have higher spatial coherence and achieve better results with the edge field. If posterior probabilities are used as training data, it may lead to a better classifier. In this way, not only can a classifier be used to improve the levelset method's outcomes, but the levelset method's higher quality training data can also be

utilized to improve the classifier. To attain better outcomes, it was decided to alternate classifier training with the levelset technique multiple times. Algorithm 2 depicts the steps of this multiphase levelset technique. During each pass, the edge field is updated according to the algorithm through suppressing spurious edges by using the most recent classifier's pixelwise probabilities. The following is a description of the algorithm:

As described in section 3, the LS Method for image segmentation can completely symbolize the segmentation contour in the form of a surface. In particular, the segmentation contour s would be zero level of the surface function. Based on [26], the deep conventional levelset can be solved using the following equation:

$$\frac{\partial \varphi}{\partial t} = g \|\nabla \varphi\| \operatorname{div} \frac{\nabla \varphi}{\|\nabla \varphi\|} + g \|\nabla \varphi\| v + \nabla g \cdot \nabla \varphi \tag{8}$$

Where, g represent the image features, which is characterized by following equation:

$$g(I, \alpha) = \frac{1}{1 + \alpha \|\nabla I\|^2} \tag{9}$$

In which, I is the smoothed image being segmented and α is the variable that can control the edge strength. Hence, it can use a finite difference scheme to solve equation (8)

$$\varphi_{t+1} = \varphi_t + \Delta t \frac{\partial \varphi}{\partial t} \tag{10}$$

Therefore, the selection of an initial surface parameter φ_0 has a significant effect in guiding the curve evolution to detect the correct segmentation as φ_0 implicitly represents the initial size, position, and the segmentation contour shape in this formulation. The levelset random in terms of position and size within the image. However, if the image is noisy or involved several different objects, setting φ_0 as broadly as possible, i.e., from the image's borders, the levelset method will be unable to segment the target object only. From this justification, the LS method is provided with a prior for the object's location and size, which could potentially improve segmentation effectiveness. Furthermore, by specifying a location prior to segmentation, the levelset method can target a specific object within the image, reducing segmentation noise.

For this model, the initial parameters φ_0 has the following function

$$\varphi_0^y = \begin{cases} 1 & \text{if } (i, J) \text{ is outside } B \\ -1 & \text{otherwise} \end{cases} \tag{11}$$

The proposed algorithm of levelset is described in follows:

Algorithm of levelset t Method
<ol style="list-style-type: none"> 1. Declarations: Image, levelset function (φ), pixelwise foreground probability (P), number of passes(n). 2. procedure levelset <ul style="list-style-type: none"> • when $n \geq 0$ $n \leftarrow n - 1$

- **Sampling of Data:**
 - Constructs the set M of random sampled pixels
 - i. **In case** $\varphi(x) \leq 0$ and when $i \in M$, added pixel x_i into the positive training set (F)
 - ii. **In other cases**, added pixel x_i into negative training set (B)
- **Updating the Classifier:**
 - i. Start Training a new probabilistic classifier by using both F and B.
 - ii. Recalculate the P value using the new classifier.
- **levelset Method:**
 - i. Reinitialize the levelset function φ using P
 - ii. Run the levelset method through using P and Φ until convergence
- 3. **end procedure**
- 4. **Output:** The label of all pixels calculated from the final levelset function

4.3 The Metrics

To evaluate the performance of the proposed model, three metrics were used : precision, recall, and F1-score. These metrics were calculated as follows []:

- **Precision:** shows how many of the data that were predicted to be positive turned out to be correct. In other words, a high level of accuracy means there are less false positives.

$$Precision = \frac{T_p}{T_p + F_p} \quad (12)$$

Where, T_p is the number of true positive, F_p is the number of false positive.

- **Recall:** The recall is the statistic that is used to determine whether the classifier is comprehensive. A lower recall rate is associated with a higher rate of false negatives, while a higher recall rate is associated with a lower false negative rate. When there is an increase in recall, there is frequently a drop in precision.

$$Recall = \frac{T_p}{T_p + F_N} \quad (13)$$

Where, F_N is the number of false negative.

- **F1-Score:** The F1-score can be calculated by taking the product of recall and precision and dividing that result by the total of recall and accuracy.

$$F1 - score = 2 \times \frac{Precision \times Recall}{Precision + Recall} \quad (14)$$

Where, F_N is the number of false negative.

5. Experimental Results

The proposed multi-stage levelset method was successfully applied to a high number of images using a PC with a CPU type Intel(R) Core(TM) i7-8550U CPU @ 1.80GHz 2.00 GHz, 20.0 GB RAM, windows 10, MATLAB 2022a. The dataset was taken from the PASCAL2 website [27]. The number of training images used was 16551 and the number of validation images was 4952. The test set was first fed into the network, which produced a classification result as well as a bounding box. Then the bounding box was fed into the levelset model. The final segmentation contour was the zero-level curve of the most recent evolution of surface parameters.

The accuracy of the proposed network is first computed on a two-dimensional irregular interface. The arbitrary values $\mu = 1 \times 10^5$, $\nu = 1$, number of epochs = 100 with 156 iterations per

epoch, and number of hidden =4 x 128 where chosen. The training took about 2 hours and 10 mins to train the network through 15600. The training loss of the proposed model through iterations is shown in Figure 6.

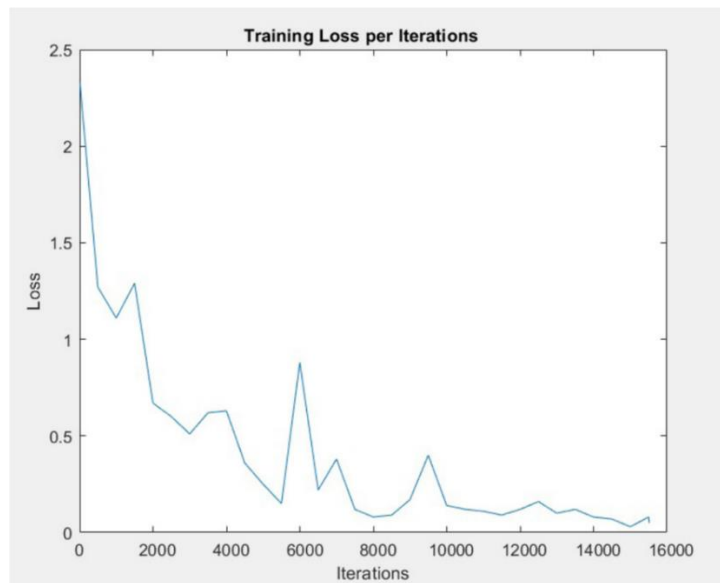


Figure 6: The training loss of the proposed model through 100epochs ((156000) iterations) From Figure 6, it can be seen that the training loss dropped from 2.4 at the first iteration of the first epoch to 0.049 at the last 15600 iteration.

Then, the metrics in section 4.3 was computed. The results show that the proposed model has achieved 94.43% in precision and 95.91% in recall %, so it got 95.16% in F1-score. Figure 7 show the area under the curve (AUC), which was used to calculate the average precision. This parameter assesses the network's performance in terms of recall and precision.

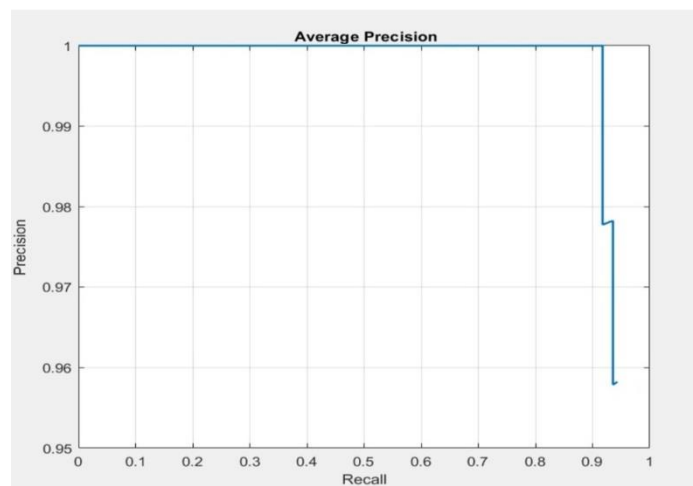


Figure 7: The training loss of the proposed model through 100epochs ((156000) iterations) When comparing the proposed model with the same CNN model without levelset, the result show that the proposed model achieved higher accuracy of 0.951 than CNN model without levelset, which achieved 0.902. Table 1 shows the testing results.

Table 1: Scores for tested results for proposed model using proposed LS algorithm compared with standard deep conventional network

Classification accuracy of proposed model	Classification accuracy of CNN model without LS
0.951	0.902

Figure 8 shows image samples that have noisy environment and the edge detection result by the proposed model.

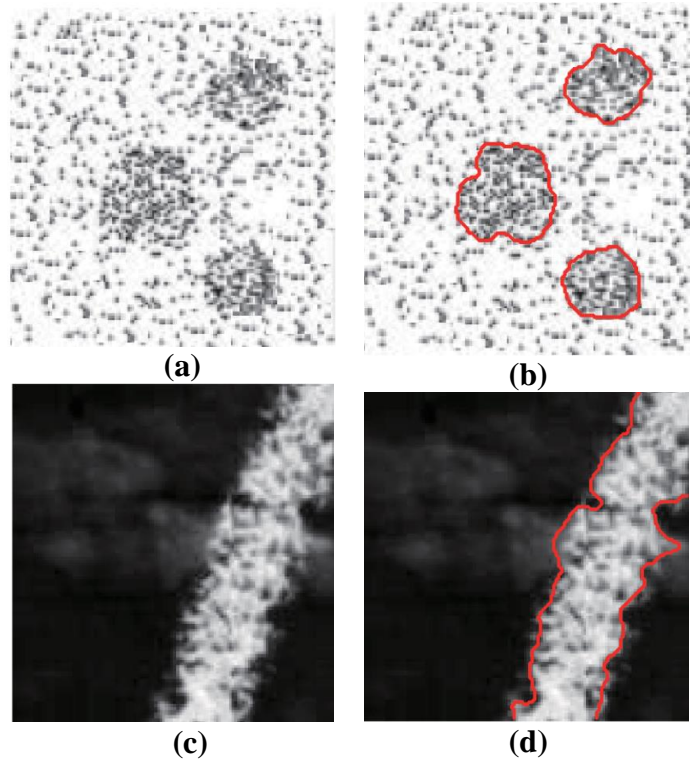


Figure 8: Two samples of biological image with noisy environment Left (a) and (c) the input images, and the right (b) and (d) are the edge detection results.

As can be seen from Figure 8, the proposed method effectively determines the edges of the desired object so it can extract features in very high detail. Figure 9 shows the extracted images from the complex background.



Figure 9: Extraction results of flower image with complex edges (a) the input images, (b) the feature extracted result

In Table 2 a comparison is presented of the proposed model with some related works mentioned in section 2. مقارنة للطرق.

Table 2: Comparison between the proposed model and some related works

Recent Works	Method	Dataset	Results
Hu et al. (2017) [19]	Deep levelset Network	SED2, PASCAL, ECSSD, OMRON, HKU-IS and THUR	For PASCAL dataset it achieved 0.136 in Mean Absolute Error (MAE) and 0.651 in F β score (A modified form of the F1 score)
Le et al (2018) [20]	Recurrent Fully Convolutional Neural Network	BRATS 2013 dataset and BRATS 2015 dataset	For BRATS 2013 dataset it achieved 0.90% in Sensitivity (Recall), 0.91 in Specificity and 0.89 in Dice (F1 Score). For BRATS 2015 dataset it achieved 0.91% in Sensitivity (Recall), 0.90 in Specificity and 0.88 in Dice (F1 Score)
Le (2018) [21]	Contextual Recurrent Residual Networks (CRRN)	Siftflow dataset and CamVid dataset	Achieved 84.7% in per-pixel accuracy (PA) and 61.0% in per-class accuracy (CA) for Siftflow dataset. And achieved 84.4% in PA and 54.8% in CA for CamVid dataset
Kim et al. (2019) [22]	Modified Approximated Heaviside Function (MAHF)	PASCAL VOC 2012	Mean Intersection-Over-Union (mIOU) = 76.5
Our Model	Deep Convolutional Neural Networks (DCNN)	PASCAL2	Achieved 94.43% in precision, 95.91% in recall %, and 95.16% in F1-score.

6. Conclusion

This study demonstrated how to optimize the Fully Convolutional Network Accuracy by integrating Deep Convolutional Neural Networks as a prior to levelset method to achieve an automatic natural image feature extraction rather than the traditional method that only incorporates uninformative prior, and it does not fine tune any hyper parameters.

From the results, we can prove that the proposed method has improved the segmentation results significantly by using prior knowledge. The Deep network in our method was found to be the lower and upper bounds, respectively, for overall precision and recall. The results show that the proposed model has achieved 94.43% in precision and 95.91% in recall %, so it got 95.16% in F1-score. In addition, when compared with model with same CNN model without levelset, the result show that the proposed model achieved higher accuracy reaching up to 0.951 that is more than CNN model without levelset that achieved 0.902.

References

- [1] R. D. Haamied, B. Q. Al-Abudi, and R. N. Hassan, "Automatic Object Detection, Labelling, and Localization by Camera's Drone System," *Iraqi Journal of Science*, vol. 62, no. 12, pp. 5008–5023, Dec. 2021, doi: 10.24996/ijs.2021.62.12.37.
- [2] M. A. A. Jabbar and A. M. Radhi, "Diagnosis of Malaria Infected Blood Cell Digital Images using Deep Convolutional Neural Networks," *Iraqi Journal of Science*, vol. 63, no. 1, pp. 380–396, Jan. 2022, doi: 10.24996/ijs.2022.63.1.35.
- [3] G. Geetha, T. Kirthigadevi, G. G. Ponsam, T. Karthik, and M. Safa, "Image Captioning Using Deep Convolutional Neural Networks (CNNs)," in *Journal of Physics: Conference Series*, Dec. 2020, vol. 1712, no. 1. doi: 10.1088/1742-6596/1712/1/012015.
- [4] I. H. Sarker, "Deep Learning: A Comprehensive Overview on Techniques, Taxonomy, Applications and Research Directions," *SN Computer Science*, vol. 2, no. 6. Springer, pp. 1–20, Nov. 01, 2021. doi: 10.1007/s42979-021-00815-1.

- [5] E. Elyan *et al.*, “Computer vision and machine learning for medical image analysis: recent advances, challenges, and way forward,” *Artificial Intelligence Surgery*, vol. 2, no. 1, pp. 24–45, Mar. 2022, doi: 10.20517/ais.2021.15.
- [6] Z. Z. Wang, “Image segmentation by combining the global and local properties,” *Expert Syst Appl*, vol. 87, pp. 30–40, Nov. 2017, doi: 10.1016/j.eswa.2017.06.008.
- [7] R. R. K. Al-Taie, B. J. Saleh, and L. A. Salman, “Image Edge-Segmentation Techniques : A Review,” *Int J Sci Res Sci Eng Technol*, vol. 8, no. 5, pp. 252–257, Oct. 2021, doi: 10.32628/ijrsrset218528.
- [8] S. Croset, J. Rupp, and M. Romacker, “Flexible data integration and curation using a graph-based approach,” *Bioinformatics*, vol. 32, no. 6, pp. 918–925, Mar. 2016, doi: 10.1093/bioinformatics/btv644.
- [9] D. Demirović, “An implementation of the mean shift algorithm,” *Image Processing Online*, vol. 9, pp. 251–268, 2019, doi: 10.5201/ipol.2019.255.
- [10] A. Joshi, M. S. Khan, A. Niaz, F. Akram, H. C. Song, and K. N. Choi, “Active contour model with adaptive weighted function for robust image segmentation under biased conditions,” *Expert Syst Appl*, vol. 175, p. 114811, Aug. 2021, doi: 10.1016/j.eswa.2021.114811.
- [11] D. Yang, Y. Du, H. Yao, and L. Bao, “Image semantic segmentation with hierarchical feature fusion based on deep neural network,” *Conn Sci*, vol. 34, no. 1, pp. 1772–1784, Dec. 2022, doi: 10.1080/09540091.2022.2082384.
- [12] P. Malhotra, S. Gupta, D. Koundal, A. Zaguia, and W. Enbeyle, “Deep Neural Networks for Medical Image Segmentation,” *Journal of Healthcare Engineering*, vol. 2022. Hindawi Limited, 2022. doi: 10.1155/2022/9580991.
- [13] E. Shelhamer, J. Long, and T. Darrell, “Fully Convolutional Networks for Semantic Segmentation,” May 2016, [Online]. Available: <http://arxiv.org/abs/1605.06211>
- [14] F. Lateef and Y. Ruichek, “Survey on semantic segmentation using deep learning techniques,” *Neurocomputing*, vol. 338, pp. 321–348, Apr. 2019, doi: 10.1016/j.neucom.2019.02.003.
- [15] X. Huang, C. Zanni-Merk, and B. Crémilleux, “Enhancing deep learning with semantics: An application to manufacturing time series analysis,” in *Procedia Computer Science*, Jan. 2019, vol. 159, pp. 437–446. doi: 10.1016/j.procs.2019.09.198.
- [16] M. Alam, J. F. Wang, C. Guangpei, L. Yunrong, and Y. Chen, “Convolutional Neural Network for the Semantic Segmentation of Remote Sensing Images,” *Mobile Networks and Applications*, vol. 26, no. 1, pp. 200–215, Feb. 2021, doi: 10.1007/s11036-020-01703-3.
- [17] Y. Liu, M. Zhu, J. Wang, X. Guo, Y. Yang, and J. Wang, “Multi-Scale Deep Neural Network Based on Dilated Convolution for Spacecraft Image Segmentation,” *Sensors*, vol. 22, no. 11, p. 4222, Jun. 2022, doi: 10.3390/s22114222.
- [18] S. B. Dilgen, “Topology and advanced shape optimization of multiphysics problems,” Ph.D. thesis, Technical University of Denmark, Kgs. Lyngby, Denmark, 2020.
- [19] P. Hu, B. Shuai, J. Liu, and G. Wang, “Deep level sets for salient object detection,” in *Proceedings - 30th IEEE Conference on Computer Vision and Pattern Recognition, CVPR 2017*, Nov. 2017, vol. 2017-January, pp. 540–549. doi: 10.1109/CVPR.2017.65.
- [20] T. H. N. Le, R. Gummadi, and M. Savvides, “Deep Recurrent Level Set for Segmenting Brain Tumors,” Oct. 2018, [Online]. Available: <http://arxiv.org/abs/1810.04752>
- [21] T. H. N. Le, C. N. Duong, L. Han, K. Luu, M. Savvides, and D. Pal, “Deep Contextual Recurrent Residual Networks for Scene Labeling,” Apr. 2017, [Online]. Available: <http://arxiv.org/abs/1704.03594>
- [22] Y. Kim, S. Kim, T. Kim, and C. Kim, “CNN-based Semantic Segmentation using Level Set Loss,” Oct. 2019, Accessed: Oct. 17, 2022. [Online]. Available: <http://arxiv.org/abs/1910.00950>
- [23] J. Park, S. M. Shontz, and C. S. Drapaca, “A Combined Level Set/Mesh Warping Algorithm for Tracking Brain and Cerebrospinal Fluid Evolution in Hydrocephalic Patients.”
- [24] M. E. Rosti, F. Picano, and L. Brandt, “Numerical Approaches to Complex Fluids,” Springer, Cham, 2019, pp. 1–34. doi: 10.1007/978-3-030-23370-9_1.
- [25] V. Lefèvre, A. Garnica, and O. Lopez-Pamies, “A WENO finite-difference scheme for a new class of Hamilton–Jacobi equations in nonlinear solid mechanics,” *Comput Methods Appl Mech Eng*, vol. 349, pp. 17–44, Jun. 2019, doi: 10.1016/j.cma.2019.02.008.

- [26] S. Gao, N. Guo, and D. Mao, "LSM-SEC: Tongue Segmentation by the Level Set Model with Symmetry and Edge Constraints," *Comput Intell Neurosci*, vol. 2021, 2021, doi: 10.1155/2021/6370526.
- [27] Z. Ding, X.-Y. Liu, M. Yin, and L. Kong, "TGAN: Deep Tensor Generative Adversarial Nets for Large Image Generation," Jan. 2019, Accessed: Oct. 22, 2022. [Online]. Available: <http://arxiv.org/abs/1901.09953>.